SLAC–PUB–9605
December 2002

Coherent Synchrotron Radiation in Storage Rings *

M. Venturini, R. Warnock, and R. Ruth
Stanford Linear Accelerator Center, Stanford University, Stanford, CA 94309

Abstract

We take a detour from the main theme of this volume and present a discussion of coherent synchrotron radiation (CSR) in the context of storage rings rather than single-pass systems. Interest in this topic has been revived by a series of measurements carried out at several light source facilities. There is strong evidence that the observed coherent signal is accompanied by a beam instability, possibly driven by CSR itself. In this paper we review a "self-consistent" model of longitudinal beam dynamics in which CSR is the only agent of collective forces. The model yields numerical solutions that appear to reproduce the main features of the observations.

To appear in the proceedings of the joint
ICFA Advanced Accelerator and Beam Dynamics Workshop
"The Physics and Applications of High Brightness Electron Beams"
Chia Laguna, Sardinia (Italy), July 1-6, 2002

*Work supported in part by Department of Energy contract DE–AC03–76SF00515.

1 Introduction

The realization of a possible role for coherent synchrotron radiation (CSR) in cyclic electron machines is old, preceding the construction of the first electron synchrotrons, and dates back at least to an unpublished paper by Schwinger[1] in 1945. Schwinger's work was motivated by concerns about energy efficiency. When passing through bending magnets charged particles radiate incoherently, with power proportional to the number of particles per bunch N, and also coherently at longer wavelengths, with power proportional to N^2. However, Schwinger[1] and others[2, 3] pointed out that unless the bunch length were exceedingly small, coherent radiation would be effectively suppressed by shielding from the metallic vacuum chamber. In spite of its more unfavorable scaling with N the coherent part of the radiation is typically a very small fraction of the overall dissipated power, and has little consequence in machine operation. As a result, interest in CSR faded somewhat after those early papers, but the subject was kept alive in several theoretical studies through the 1960's and 1970's (see the bibliography in the first paper of Ref. [4]). There was interest at Berkeley [5], Dubna [6], and elsewhere in connection with the "smoke ring" acceleration concept. It was not until the mid 1980's that the first experimental indications[7, 8] of CSR were reported, and 1989 that the first clear observation was made, by Nakazato *et al.* [9]. The latter involved a linac and a bending magnet, rather than a circular machine. Only in recent years detection of CSR from storage rings has been more conclusively established through a series of measurements carried out at NIST[10] (Maryland), NSLS[11, 12, 13] (Brookhaven), MAX Laboratory[14] (Lund, Sweden), BESSY[15] (Berlin), and ALS[16] (Berkeley). The renewed attention to CSR stems in part from the prospect of exploiting the process to create a new class of high-power light sources in the infrared region. A first suggestion of the practical implications of CSR was contained in a paper by Michel[18] in 1982. Later, a detailed proposal was made by Murphy and Krinsky[19], and the design of a dedicated CSR source is currently being explored at LBNL[17] (Berkeley).

As this volume well illustrates, CSR has been gaining increasing attention because of its potential role as a mechanism for driving collective instabilities. While at present not a factor limiting beam quality in storage rings (a marked difference from the case of bunch compressors in FEL applications), CSR instabilities are nonetheless important as they appear to be connected with most of the above observations [10, 11, 12, 13, 14, 15, 16]. Two fea-

tures in these measurements indicate a connection: the existence of a current threshold for detecting a coherent signal and a radiation wavelength considerably shorter than the nominal bunch length. In particular, the latter implies that the bunches carry a modulation in the longitudinal distribution. This is because, in general, coherent radiation at a wavelength λ can be emitted only if the Fourier spectrum of the longitudinal charge density in the bunch is significant at that λ (if λ is sufficiently small the shielding by the vacuum chamber becomes ineffective and a coherent signal can be detected). The required modulation could naturally be provided by a collective instability. There is an on-going debate about whether the cause of such an instability might be the machine geometric impedance or, as recently suggested by Heifets and Stupakov[20], the CSR process itself. Perhaps the most convincing argument in favor of the latter hypothesis is the apparent generality of coherent emissions, which have been detected over a number of very different machines. In addition, there appears to be a substantial agreement so far between predictions by the standard linear theory of collective instabilities applied to CSR and observations.

In this paper we review some recent work[21, 22] that we have undertaken to study the interplay between the coherent radiation process, the longitudinal beam dynamics, and related instabilities. The goal is to go beyond linear theory, hoping to explain aspects of the observations that cannot be captured otherwise. For example, in most of the current observations of CSR in storage rings, a typical signal presents a bursting time structure. Radiation appears in recurrent short peaks separated by relatively long intervals, some fraction of the damping time. Details like the separation between the peaks and the amount of radiation released at each burst depend on the beam current. Smaller currents are typically associated with more regular patterns of emission. A linear theory can explain the onset of the instability generating the emission but not the time structure of the ensuing signal.

We proceed to a numerical solution of the fully nonlinear 1-D Vlasov-Fokker-Planck (VFP) equation for the bunch distribution in phase space. The model is "self-consistent", as it includes the distribution-dependent collective force associated with CSR. With the representation of the CSR-induced collective force that will be discussed in the next Section, the resulting solutions appear to reproduce all the qualitative features of the coherent signal found experimentally. Since the only collective force in the model is from CSR, the result is an argument in favor of the idea that the machine geometric impedance plays at most a secondary role. Nevertheless, it will still

be interesting in further work to assess the role of the geometric impedance, which may vary from one machine to another.

2 The model

Our model is based on the usual one-dimensional longitudinal motion under linear r.f. focusing, with radiation damping and quantum fluctuations from incoherent emission of photons [24]. To this we add a "self-consistent" account of the nonlinear interplay of CSR and particle dynamics, based on the Vlasov-Fokker-Planck (VFP) equation for the phase space distribution.

In the ultra-relativistic limit, which is of interest here, the Lorentz factor γ is much larger than unity and $\alpha \gg 1/\gamma^2$, so that the momentum compaction α is about the same as the slippage factor. It is convenient to work with the dimensionless phase space variables, $q = z/\sigma_z$ and $p = -\Delta E/\sigma_E$, where z is the distance from the test particle to the synchronous particle (positive when the test particle leads), and $\Delta E = E - E_0$ is the deviation of energy from the design energy. Normalization is by the low-current r.m.s. bunch length and energy spread, which are related by the equation $\omega_s \sigma_z / c = \alpha \sigma_E / E_0$, where ω_s is the angular synchrotron frequency. In these coordinates the unperturbed equations of motion are $dq/d\tau = p$, $dp/d\tau = -q$, with time variable $\tau = \omega_s t$.

The VFP equation for the phase-space distribution function $f(q, p, \tau)$ is

$$\frac{\partial f}{\partial \tau} + p\frac{\partial f}{\partial q} - \left[q + I_c F(q, f, \tau)\right] \frac{\partial f}{\partial p} = \frac{2}{\omega_s t_d} \frac{\partial}{\partial p} \left(pf + \frac{\partial f}{\partial p} \right), \tag{1}$$

where $-I_c F(q, f, \tau)$ is the collective force due to CSR, in principle the longitudinal electric field obtained from Maxwell's equations with charge/current densities derived from f itself. The nonlinear Vlasov operator on the left side accounts for the complicated short term dynamics, while the Fokker-Planck operator on the right side accounts for long-term effects of incoherent radiation: damping, and diffusion due to quantum fluctuations. The longitudinal damping time is t_d. We normalize F so that the current parameter is $I_c = e^2 N/(\omega_s T_0 \sigma_E)$, where N is the bunch population and T_0 is the revolution time.

Since it is difficult to solve the Maxwell equations with a realistic representation of particle orbits and vacuum chamber walls, we compute the collective force as though it came from a simple model which is meant to express the essential features. The vacuum chamber is represented by infinite parallel

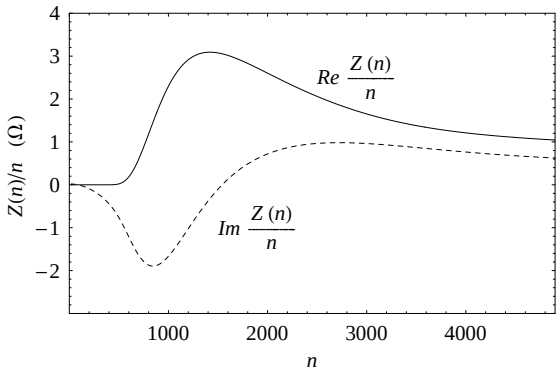

Figure 1: Real (solid line) and imaginary (dashed line) parts of $Z(n)/n$ in ohms. Parallel-plate model with $h = 4.2$ cm, $R = 1.9$ m, and $E_0 = 737$ MeV.

plates, perfectly conducting, with vertical separation h. The particles move on circular orbits of fixed radius R. In cylindrical coordinates (r, θ, y), with y-axis normal to the plates and origin in the midplane, the charge density has the form $\rho(r, \theta, y, t) = eN\lambda(\theta - \omega_0 t, t)H(y)\delta(r - R)/R$, where $\omega_0 = \beta_0 c/R$ is the revolution frequency of the circular model (not of the actual ring). The vertical density $H(y)$ is fixed; we choose H to be constant for $|y| < \delta h/2$, and 0 otherwise. The longitudinal density in the beam frame evolves by VFP dynamics through the relation $\lambda(\theta, t) = (R/\sigma_z) \int f(R\theta/\sigma_z,\ p,\ \omega_s t)dp$.

The radius R is identified as the radius of curvature in the bending magnets, not the average geometrical radius, of the actual ring. Thus, we effectively neglect transient effects as the particles enter and leave bends, hoping that at least the total work done by the CSR force over a turn will be approximated by the model. The plate separation is taken to be the average height of the actual vacuum chamber in the bends. The parameters entering the unperturbed equations of motion will be those of the actual ring. Only the CSR force is computed as though the trajectory were circular.

We define $E(\theta, t) = \int e_\theta(\theta, R, y, t)H(y)dy$ to be the longitudinal electric field averaged over the transverse distribution. The double Fourier transform (FT) of the field is $\hat{E}(n, \omega) = (2\pi)^{-2} \int d\theta \int dt \exp(-in\theta + i\omega t)E(\theta, t)$, which is related to the corresponding FT of the current I through the impedance: $-2\pi R\hat{E}(n, \omega) = Z(n, \omega)\hat{I}(n, \omega)$. The impedance is given by [4]

$$\frac{Z(n,\omega)}{Z_0} = \frac{(\pi R)^2}{\beta_0 h} \sum_{p=1,3,\cdots} \Lambda_p \left[\frac{\omega\beta_0}{c} {J_n}' {H_n^{(1)}}' + (\frac{\alpha_p}{\gamma_p})^2 \ \frac{n}{R} \ J_n H_n^{(1)} \right]. \qquad (2)$$

Here $H_n^{(1)} = J_n + iY_n$, where J_n and Y_n are Bessel functions of the first and second kinds, respectively, evaluated at $\gamma_p R$, with $\alpha_p = \pi p/h$, $\gamma_p^2 = (\omega/c)^2 - \alpha_p^2$, $\Lambda_p = 2(\sin x/x)^2$ and $x = \alpha_p \delta h/2$. In MKS units $Z_0 = 120\pi\ \Omega$. The sum over positive odd integers p arises from a Fourier expansion with respect to y.

We suppose that during the i-th time step $t_i \rightarrow t_i + \delta t$ in integration of (1) the bunch can be considered as rigid. Next, we assume that during that time step the CSR force can be computed as though the bunch had its present form for all time. In that case we get the field from the source $\hat{I}(n,\omega) = eN\omega_0\lambda_n(t_i)\delta(\omega - n\omega_0)$, where $\lambda_n(t_i) = (1/2\pi)\int d\theta \exp(-in\theta)\lambda(\theta, t_i)$. Then only the "diagonal" part of the impedance, $Z(n) = Z(n, n\omega_0)$, enters the picture. The inverse FT gives the collective force for (1) through $F(q, f(\tau_i)) = -\omega_0 \sum_n \exp(inq\sigma_z/R) Z(n) \lambda_n(t_i)$. The real part of $Z(n)/n$ has a peak value of about $132h/R\ \Omega$ and is negligible for $n < n_0 = \pi(R/h)^{3/2}$. Fig. 1 shows the real and imaginary parts of $Z(n)/n$ for a choice of parameters meant to model the NSLS VUV Storage Ring.

A more exact treatment of bunch deformation in the impedance picture, accounting strictly for causality and retardation, involves off-diagonal contributions of $Z(n,\omega)$. This matter will be discussed elsewhere [22], as will our procedure for fast evaluation of the FT defining $\lambda_n(t_i)$.

3 A Case Study: the NSLS VUV Storage Ring

In the following we show examples of solutions to Eq. (1) that are meant to model the beam dynamics for some typical setting of the Brookhaven NSLS VUV Storage Ring. We chose to refer to this machine mostly because of the extensive measurements of CSR that have been carried out over the past few years [11, 12, 13]. The VUV Ring has a double-bend achromat lattice with a local radius of curvature $R = 1.9$ m and a vacuum chamber size $h = 4.2$ cm. The list of other relevant parameters includes a synchrotron frequency $\omega_s/2\pi = 12$ kHz; revolution frequency $1/T_0 = 5.9$ MHz; damping

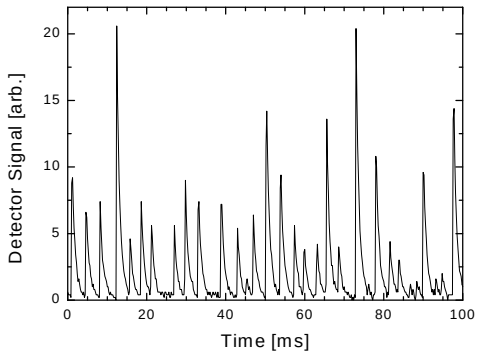

Figure 2: Far infrared detector output with emission bursts at the NLSL VUV Ring. (Courtesy of G. Carr.)

time $t_d = 10$ ms; energy $E_0 = 737$ MeV. The rms bunch length corresponding to the natural energy spread of $\sigma_E/E_0 = 5 \times 10^{-4}$ is $\sigma_z = 5$ cm.[†] During CSR measurements the VUV ring was operated in a single-bunch mode. In this regime the ring supports a current up to 400 mA, corresponding to $N = 4 \times 10^{11}$ particles. The experimental current threshold for detection of coherent signal for the particular setting under consideration here is 100 mA. This can be changed considerably through variations of the machine momentum compaction[11].

Figure 2 shows an example of a coherent signal in the far infrared with a characteristic bursting structure (from G. Carr *et al.*[11]). In this particular instance the peaks are separated by a few msec and appear to have a fairly regular spacing. The duration of the peaks is dominated by the thermal time constant of the detector (about $200\mu s$[11]).

4 Linear Theory

Linearization of Eq. (1) can be used to obtain useful information regarding the conditions for the onset of the instability. As we neglect the effects of the geometric machine impedance, a Gauss distribution $f_0 = e^{-(p^2+q^2)/2}/(2\pi)$

[†]For beam height δh, which is not a critical parameter, we take 0.1 mm.

in energy spread and spatial variable is a very good approximation to an equilibrium. For bunched beams the linear equation obeyed by f_1, a small deviation about equilibrium, is still too complicated to have a solution in closed analytical form. However, under the conditions that the instability be fast and the wavelength of the unstable mode small compared to bunch size one can use the linearized Vlasov equation for a coasting beam (*i.e.* neglect the rf focusing term proportional to q) . The current carried by the coasting beam should be the same as the peak current for the bunched beam (Boussard criterion). The modified linear equation admits wave solutions with space-time dependence $\exp[i(nq\sigma_z/R - \nu\tau)]$ yielding the dispersion relation

$$\frac{I_c\omega_0 R^2}{\sqrt{2\pi}\sigma_z^2}\frac{Z(n)}{n} = \frac{i}{D(\nu R/\sigma_z n)}, \tag{3}$$

where $D(z) = 1 + iz\sqrt{\pi/2}w(z/\sqrt{2})$ and $w(z) \equiv e^{-z^2}\mathrm{erfc}(-iz)$ is the error function of complex argument[24]. Analysis of the dispersion relation is best represented on a Keil-Schnell diagram by plotting the LHS part of Eq. 3 for a given current I_c and all harmonic numbers n; see Fig. 3. If the current is sufficiently large these curves cut through the stability boundary (dashed line in Fig. 3) and unstable solutions (with Im $\nu > 0$) emerge. From this analysis one finds a current threshold $I_c > I_c^{th} = 6.2$ pC/V, corresponding to a single-bunch circulating current of 168 mA or $N = 1.8 \times 10^{11}$. Close to threshold the wavelength of the most unstable mode is $\lambda = 2\pi R/n = 6.8$ mm with $n = 1764$. These values are reasonably close to the observed wavelength $\lambda = 7$ mm and critical current 100 mA for detection of a coherent signal [11]. The linear theory also indicates that the instability is very fast: the exponential growth-time of the most unstable mode is as low as one tenth of synchrotron period even for a current only 5% above threshold – validating the use of the Boussard criterion. This linear analysis is essentially the same as the one worked out by Heifets and Stupakov[20]. The only difference is that there the radiation impedance is relative to free space – implying that the result is meaningful only when the calculated unstable wavelength is below the shielding cutoff. A linear analysis for a bunched beam [23], with the radiation impedance for a resitive toroidal vacuum chamber, indicated some time ago that CSR alone could cause an instability at plausible current, at least for parameters of a compact storage ring [19].

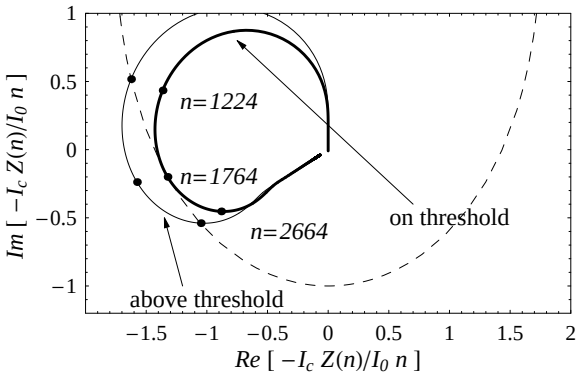

Figure 3: Keil-Schnell diagram for the linear motion of the NSLS VUV Ring. The dashed line is the familiar onion-shaped stability boundary for Gaussian equilibria. The thick line corresponds to the current (parameter) threshold $I_c = 6.2$ pC/V; $I_0 = \sqrt{2\pi}\sigma_z^2/\omega_0 R^2$.

5 Numerical Results

Above current threshold for instability, the numerical solutions of Eq. (1) present a characteristic sawtooth behavior that sets in after a transient depending on the initial condition. The pattern is evident from the plot of the rms bunch length versus time shown in Fig. 4 (picture on the left). The corresponding solution was obtained for a value $I_c = 10.5$ pC/V of the current parameter (equivalent to 3×10^{11} particles/bunch) starting from a slightly perturbed gaussian distribution. The thickness of the curve is due to the fast oscillation of the quadrupole mode.

The cycle of the sawtooth pattern follows a sequence: instability $\rightarrow$ saturation $\rightarrow$ damping. Close inspection of the solutions shows that where the envelope of the bunch length oscillation is minimum, a ripple (microbunching) appears on top of the charge distribution, see Fig. 5, right picture. This is the point where the density of the distribution in phase space is the largest and one may expect that the conditions for the collective instability are met. As predicted by the linear theory, the amplitude of this modulation grows rapidly. In the process the distribution function experiences a sudden enlargement as reflected by jumps in the evolution of either the rms bunch length (see picture) or energy spread. Next, as the density of the distribution in phase space decreases and reaches some critical value, saturation of the instability follows. This is where the effect of radiation damping starts to

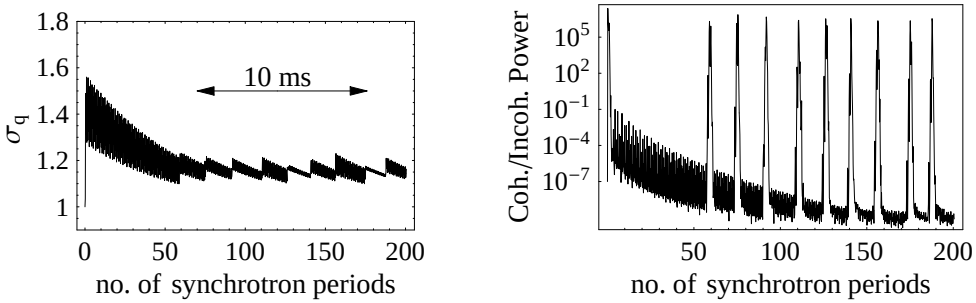

Figure 4: On the left: rms bunch length (normalized coordinates) vs. number of synchrotron periods. On the right: ratio of coherent radiation power to incoherent power vs. number of synchrotron periods for a narrow band of modes about a wavelength $\lambda = 7$ mm. In both cases $I_c = 10.5$.

become apparent. It causes the bunch distribution to slowly shrink until the conditions for instability are met again so that the cycle can repeat itself.

Emission of coherent radiation takes place in correspondence to the appearance of microbunches, at the notches of the bunch length envelope. The time structure of the signal follows naturally that of the sawtooth pattern. The expected coherent radiation emitted at the $n-$th harmonic is given by

$$P_n^{coh}(t) = 2(eN\omega_0)^2 \mathrm{Re}Z(n)|\lambda_n(t)|^2 \tag{4}$$

where λ_n is the Fourier component of the (normalized) charge density (see Section 2). By comparison the incoherent part of radiation is expressed by $P_n^{incoh} = 2N(e\omega_0)^2 \mathrm{Re}Z(n)/(2\pi)^2$. Plot of the coherent-to-incoherent-power ratio for a narrow band of modes around the wavelength $\lambda = 7$ mm is reported in Fig. 4 (picture to the right).

In qualitative agreement with the experimental observations the pattern of bursts is fairly regular for moderate currents while for larger current more stochastic features start to appear – both in the occurrence of the bursts as well in their peak values. Moreover, we found a dependence of the average separation between bursts on the current, again in qualitative agreement with observations[25]. A plot of the average separation between bursts vs the current parameter I_c is reported in Fig. 5 (picture to the right).

In solving Eq. (1) as a time-domain initial-value problem we used a variant of the Perron-Frobenius method presented by R. Warnock and J. Ellison[26]. This involves a representation of the distribution function f on a cartesian

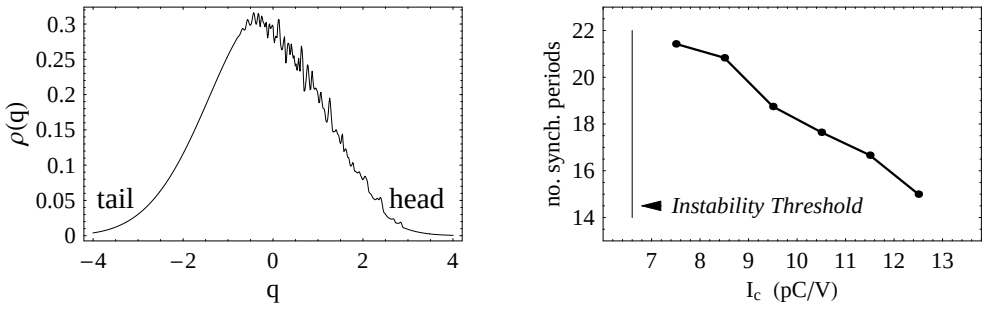

Figure 5: On the left: snapshot of the charge distribution with microbunching taken during a radiation burst ($I_c = 12.5$ pC/V). On the right: plot of average burst separation vs. current parameter.

grid and propagation of the derivatives $\partial_q f$ and $\partial_p f$ along with f. A more detailed description will be found a forthcoming publication[22].

6 Conclusions

CSR has become a very active subject of research over the past few years. While most of the attention is presently devoted to CSR effects in single-pass systems, we hope to have shown their relevance in storage rings as well. The basic physics of the instability caused by CSR is identical in both cases and its basic signature, *i.e.* the existence of microbunching, is also the same. However, while CSR-driven microbunching has been observed in bunch compressors both in simulations and in direct measurements, at this time there is no direct experimental evidence of it in storage rings (*e.g.* from streak camera measurements). The evidence is indirect through the detection of a coherent signal.

Numerical integration of our dynamical model supports the notion that the collective instability caused by CSR alone is sufficient to account for microbunching. In addition, the model appears to reproduce at least qualitatively the main features of the observations: the existence of a current threshold for detection of CSR, the wavelength at the peak of the coherent radiation spectrum, and the time structure of the signal characterized by short recurrent bursts separated by a substantial fraction of the damping time.

It is in our plans for the future to explore extension of the VFP solver

to include the horizontal degree of freedom. If successful, such an extension could provide an interesting alternative to the macroparticle methods currently used to study beam propagation through bunch compressors.

Acknowledgments

We benefitted from discussions with K. Bane, J. Byrd, A. Chao, J. Ellison, P. Emma, S. Heifets, Z. Huang, S. Kramer, S. Krinsky, J. Murphy, B. Podobedov, F. Sannibale, and G. Stupakov. Work was supported in part by DOE contract DE-AC03-76SF0051.

References

[1] J. Schwinger, unpublished (1945) [transcribed in LBL report LBL-39088 (1996)].

[2] L. Schiff, Rev. Sci. Instr., **17** no. 1, 6 (1945).

[3] J. Nodvick and D. Saxon, Phys. Rev. **96**, 180 (1954).

[4] R. Warnock and P. Morton, Part. Accel. **25**, 113 (1990); R. Warnock, SLAC reports SLAC-PUB-5375 (1990), -5417 (1991), -5523 (1991).

[5] D. Keefe *et al.*, Phys. Rev. Lett. **552**, 558 (1969); A. Faltens and L. J. Laslett, Part. Accel. **4**, 151 (1973); V. Brady, A.Faltens, and L. J. Laslett, LBL report LBID-536, 1981.

[6] A. G. Bonch-Osmolovskii and E. A. Perel'shtein, Izv. Rad. Phys. **8**, 1080 (1970); *ibid.* **8**, 1089 (1970); B. G. Shchinov *et al.*, Plasma Physics **15**, 211 (1973).

[7] J. Yarwood *et al.*, *Nature* **312**, 742 (1984).

[8] E. Schweizer, *et al.*, Phys. Res. Sect. A **239**, 630 (1985).

[9] T. Nakazato *et al.*, Phys. Rev. Lett. **63**, 1245 (1989).

[10] U. Arp *et al.* Phys. Rev. ST Accel. Beams **4**, 054401 (2001).

[11] G. Carr, S. Kramer, J. Murphy, R. Lobo, and D. Tanner, Nucl. Instr. Meth. Phys. Res. Sect. A **463** 387-392 (2001).

[12] B. Podobedov *et al.*, Proc. 2001 IEEE Part. Accel. Conf., p. 1921 (IEEE, Piscataway NJ, 2002).

[13] S. Kramer *et al.*, Proc. 2002 Euro. Part. Accel. Conf., to be published; S. Kramer, Phys. Rev. ST Accel. Beams **5**, 112001 (2002).

[14] Å. Anderson, M. Johnson, and B. Nelander, Opt. Eng. **39**, 3099 (2000).

[15] M. Abo-Bakr, J. Feikes, K. Holldack, G. Wüstefeld, and H.-W. Hübers, Phys. Rev. Lett. **88**, 254801-1 (2002).

[16] J. M. Byrd *et al.*, Proc. 2002 Euro. Part. Accel. Conf., to be published.

[17] W. C. Barry *et al.*, Proc. 2002 Euro. Part. Accel. Conf., to be published.

[18] F. Michel, Phys. Rev. Lett. **48** 580 (1982).

[19] J. B. Murphy and S. Krinsky, Nucl. Instr. and Methods in Phys. Res. A **346** 571 (1994)

[20] S. Heifets and G. Stupakov, Phys. Rev. ST Accel. Beams **5**, 054402 (2002).

[21] M. Venturini and R. Warnock, Phys. Rev. Lett. **89**, 224802 (2002).

[22] M. Venturini, R. Warnock, and R. Ruth, to be submitted to Phys. Rev. E.

[23] R. Warnock and K. Bane, SLAC report SLAC-PUB-95-6837 (1995).

[24] S. Y. Lee, *Accelerator Physics*, Chap. 3 (World Scientific, Singapore, 1999).

[25] B. Podobedov, Private communication.

[26] R. Warnock and J. Ellison, in *The Physics of High Brightness Beams*, (World Scientific, Singapore, 2000).